Highly enhanced electrochemical performance of novel based electrode materials for supercapacitor applications: an overview.

RAMACHANDRAN, R., CHEN, T.-W., CHEN, S.-M., RAJA, P., FERNANDEZ, C., RANI, S.D., GAJENDRAN, P., RAJU, G., BASKAR, T. and JEYAPRAGASAM, T.

2019

Int. J. Electrochem. Sci., 14 **(2019)** 1634 – 1648, doi: 10.20964/2019.02.75

International Journal of ELECTROCHEMICAL SCIENCE
www.electrochemsci.org

Mini Review

Highly Enhanced Electrochemical Performance of Novel based Electrode Materials for Supercapacitor Applications – An Overview

Rasu Ramachandran[3,], Tse-Wei chen,[1,2], Shen-Ming Chen[1,*], Paulsamy Raja[4], Carlos Fernandez[5], Selvarajan Divya Rani[3], Pandi Gajendran[3], Ganapathy Raju[6],Thangaraj Baskar[7],Tharini Jeyapragasam[8]*

[1]Electroanalysis and Bioelectrochemistry Lab, Department of Chemical Engineering and Biotechnology, National Taipei University of Technology, No.1, Section 3, Chung-Hsiao East Road, Taipei 106, Taiwan, ROC.
[2]Research and Development Center for Smart Textile Technology, National Taipei University of Technology, Taipei 106, Taiwan, ROC.
[3]The Madura College, Department of Chemistry, Vidya Nagar, Madurai – 625 011, Tamil Nadu, India.
[4]Vivekananda College of Arts and Science, Agastheeswaram, Kanyakumari – 629 004, Tamil Nadu, India.
[5]School of Pharmacy and Life Sciences, Robert Gordon University, Aberdeen (UK) – AB107GJ.
[6]Department of Zoology, Pioneer Kumaraswamy College, Nagercoil – 629 003, Tamil Nadu, India.
[7]School of Food and Biological Engineering, Jiangsu University, Zhenjiang -212013, Jiangsu province, P.R.China.
[8]Sethu Institute of Technology, Pulloor – 626 115, Kariapatti, Tamil Nadu, India.
Corresponding Authors:
[*]E-mail: smchen78@ms15.hinet.net (S.-M. Chen), ultraramji@gmail.com (R. Ramachandran)

Received: 5 November 2018 / *Accepted:* 14 December 2018 / *Published:* 5 January 2019

The research and recent progress of electrochemical energy storage devices applied to various applications during the past two decayed are reviewed. Different electrode materials (carbon-based materials, metal oxides, conducting polymers, metal nanoparticles and nanocomposites), can be used as the most important features for supercapacitors. Recently, research efforts of supercapacitor electrodes have been used to increase the specific capacitance and its cyclic stability. In this review designate current efforts energy storage preparation methods, materials and different morphological structure for electrochemical capacitor applications. The principle of design, extended surface area, improve the capacitance properties and long-durability of the electrochemical capacitor are discussed.

Keywords: Nanocomposite, Morphology, Electrochemical properties, Ultracapacitors, Electrode stability.

1. INTRODUCTION

The nanomaterial is a promising electrode materials device, which has received a significant interest of various applications, such as electrochemical sensors [1], biosensors [2], energy storage devices (fuel cells, batteries and supercapacitors) [3-5] and gas sensor [6]. Among these, the supercapacitor is one of the energy storage devices, able to store the energy in electrode/electrolyte interface by electrode surface area [7]. An ultracapacitor, an extensive energy storage device for the application of low cost, environment-friendly and improved their power density, long-durability and excellent cyclic stability during the charge-discharge process [8]. Supercapacitors exhibit several advantages than the other energy storage devices (batteries and fuel cells), the deficiencies of high power density and long cycle life [9]. Recently, many researchers have focused on novel electrode materials (carbon fibre, carbon nanotubes, fullerene, graphene oxide and nanocomposites) received considerable attention due to their electrode various unique structures, porosity and a large surface to volume ratio for the storage of energy devices [10-14].

Tan *et al* [15] synthesized a high conductive and suitable pore distributed ultrathin nitrogen doped graphite carbon nano capes *via* a simple template route. The structurally CNCs-800 showed a great pseudocapacitance (248 F g^{-1} @ 1.0 Ag^{-1}) and outstanding cyclic stability (5000 cycles) in 6M KOH solution. Recently, Higgins *et al* [16] fabricated a carbon nanotube-based MnO_2 composite, which displayed the reasonable specific capacitance (~42 F g^{-1}). Pseudocapacitors are mainly studying through metal oxides and conducting polymer materials, able to provide more capacitance values than the electrical double-layer capacitance (carbon-based materials). Nano-based novel electrode materials have been used as the key component for the formatting of the specific capacitance values. Besides, one of the important morphological studies has been highlighted such as tubes, rods, spheres and flowers etc. The size-controlled morphological electrode materials have great advantages for electrochemical energy storage devices. Hierarchically porous carbons (HPCs) have been synthesized by a sol-gel method; however, they were exhibited highest specific capacitance value of 60.6 F g^{-1} in 6.0M KOH medium [17]. Despite, a major part of available defects sites have been extensively studied for enhancing specific capacitance properties, due to stacking and aggregation between the electrodes and electrolytes [18]. Fang *et al* [19] developed novel asymmetric all-solid-state paper supercapacitors (APSCs) have a great attention because of their outstanding electrochemical properties (energy device), lightweight, high power density and outstanding electrochemical stability. On the other hand, a hierarchical nanostructure of earth-abundant ZnV_2O_4 (several oxidation states) was synthesized and made the remarkable performance of energy storage device (360 F g^{-1} @ 1 Ag^{-1}) with good stability (1000 cycles) [20]. High-performance supercapacitor holding the practical applications in promising and portable energy storage devices are developed recently [21-23]. Kim *et al* [24] fabricated silicon carbide microsphere supported birnessite type MnO_2 (SiC/B-MnO*x*) composite by new approach method, with a specific capacitance value of 251.3 F g^{-1} @ 10 mV s^{-1}. Meng and co-workers [25] reported the 3D SnO_2 nanoflowers on titanium foil using a simple hydrothermal method without any surfactant/catalyst. Moreover, nickel cobalt double hydroxide nanoflowers have been widely used as an asymmetric (pseudo capacitive) super capacitive behaviour, the electrode material exhibited high specific capacitance [26]. Hsu *et al* [27] employed the electrospinning preparation of uniform

distributed poly(acrylonitrile-co-butadiene) (PAN-Co-PB) in electrospun fibre. The interconnected carbon nanofiber could increase in both electrical conductivity and showed the good cyclic stability of energy storage. Porous activated carbon fibre (ACF) electrode material is another option for electrical double layer capacitance due to their high surface to volume ratio and exhibit reasonable specific capacitance (173 F g^{-1}) value [28].

This review article is explored on various synthesis routes of nanomaterials and modified with carbon materials, metals, metal oxides and conducting polymer for the formation of the nanocomposite. However, a special kind of attention also to be highlighted in the experimental technique and relating mechanism to the basis of supercapacitor (specific capacitance) behaviour. This article is overviewed past, present and future research based development of ultracapacitors are discussed in terms of novel electrode materials. Recently, researchers are focused on nanocomposite and three-dimensional based electrode materials are already drawn from a wealth of research activities, versatile unique properties and many electrochemical applications. The data for the selective discussion of various electrode materials are listed in Table.1 and it summarized various methods, electrode materials, surface area, power density, energy density, specific capacitance and finally the cyclic stability of the fabricated/deposited electrode materials.

Table 1. The supercapacitor properties of different electrode materials

S. No	Electrodes materials	Methods	Surface Area (m^2 g^{-1})	Morphology	Energy Density (Wh kg^{-1})	Power density (W kg^{-1})	Specific capacitance (F g^{-1})	Stability (Cycles)	Ref
1	$Ni_xCo_{(1-x)}(OH)_2$	Hydrothermal	162.3	Nano flake	19.4	80.5	206.7 mA hg^{-1}	4000	[29]
2	Polyacrylonitrile/ Poly(methyl methacrylate)/ Graphene	Electrospinning	500	Nanofiber	16-21	400-20,000	128	100	[30]
3	Carbon fiber paper/Cobalt oxide	Tailored Architecture	-	Nano net	-	-	1124	5000	[31]
4	Ni_3S_2/Carbon	Hydrothermal	506	Nanofiber	25.8	425	883	2500	[32]
5	Bi_2S_3/Graphene composite	Precipitation	29	Nano rod	-	-	290	500	[33]
6	Cobalt oxy hydroxide (CoOOH)	Hydrothermal	57	Nano rod	7	800	198	5000	[34]
7	Nitrogen doped carbon	Chemical	1322	Nano porous	-	-	564.5	5000	[35]

2. DIFFERENT ELECTRODE MATERIALS FOR SUPERCAPACITORS

2.1. Supercapacitors based on carbon electrode materials

Reduced graphene oxide has been used as an environmentally friendly, high performance transparent and flexible electrode catalyst of energy storage devices for future consumer electronics.

The different morphological device provided high mechanical flexibility and exhibited better capacitive performance [36]. An *et al* [37] have recently developed a stable non-covalent functionalization of graphene (Single, few and multi-layered graphene flake) with 1-pyrene carboxylic acid. The exfoliated single, few and multi-layered graphene flake stable in aqueous dispersion and it would pave the way of direct ultracapacitor development. Despite their advantages, three-dimensional graphene aerogel-nickel foam (GA@NF) hybrid based electrode can exhibit hierarchical porosity, high conductivity and it can extensively be studied as a novel electrode for supercapacitor [38]. Novel ultrathin nitrogen-doped graphitic carbon nanocages most valuable advance electrode materials used for supercapacitor with moderate graphitization, high surface area, good mesoporosity and excellent rate capability [39]. The use of renewable macroporous carbon-based materials, three-dimensional (3D) interpenetrating macro porous morphology as electrode support is attractive for supercapacitor. The template-free macroporous carbons enable, they exhibited outstanding capacitance performance of 330 F g^{-1} and good cyclic stability (1000 cycles) during the charging-discharging processes [40].

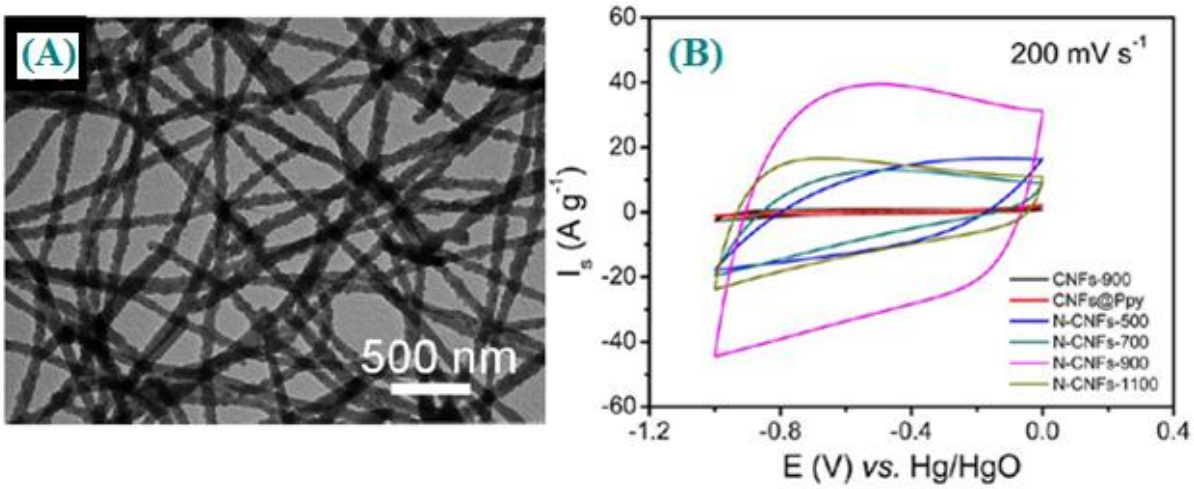

Figure 1. ("Reprinted with permission from (*ACS Nano 6 (2012) 7092-7102*). Copyright (2012) American Chemical Society") Ref [41].

Figure.1.(A) shows high-resolution TEM image smooth morphological surfaces of CNFs@Ppy, the surfaces of CNF were deposited on the Ppy surface quite small and Fig.1(B) discussed the different exhibited remarkable electrochemical properties at various electrodes [41]. The hierarchical graphene-based MnO_2-coated carbon nanotubes (MnC/RGO) composite have been extensively investigated by cyclic voltammetry, galvanostatic charge-discharge and electrochemical impedance spectrometry. The composite has received great interest because of their maximum specific capacitance value of 193 F g^{-1}[42]. The conductive of two-dimensional (2D) MnO_2 nanoplatelets are enhanced by the addition of carbon nanotubes, which provided high capacitance up to 40 times than the bare MnO_2 [43].

2.2. Supercapacitors based on metal oxide electrode materials

Metal oxide nanoparticles have been exploited as potential electrode materials, due to their high surface area, high power density, fast charge-discharge and long durability of the energy storage

devices. The performances of electrochemical silicon carbide microsphere-based birnessite MnO_x (SiC/MnO_x) supercapacitors, however, need to be improved for their electrical conductivity, the effective interfacial area between MnO_x and the supporting electrolyte [44]. Commonly, ZnO/NiO core-shell composites have been widely used as the supercapacitors electrode materials. They have achieved a maximum specific areal capacitance (4.1 F cm^{-2}) and long-term cyclic stability (4000 cycles) [45]. Currently, a rapid and template-free microwave-assisted heating reflux methods have been used for the synthesis of a three-dimensional hierarchical flower shaped $NiCo_2O_4$ microsphere electrode. The as-fabricated electrodes are narrow pore size distribution (5-10 nm) and showed high specific capacitance (1006 F g^{-1} @ 1 Ag^{-1}) [46]. Metal oxide ($W_{18}O_{49}$) and polyaniline (PANI) based electrodes have electronic, electrochemical, optical and electrocatalytic properties with fascinating features [47]. Furthermore, a simple hydrothermal method preparation of highly conductive of 3D graphene modified with cobalt oxide electrode is also demonstrated that capable of delivering high specific capacitance (~1100 F g^{-1}) [48]. Among these, graphite/PEDOT/MnO_2 composite represents the state-of-the-art as a flexible electrode, because of their high performance of supercapacitors and achieved high energy (31.4 Wh kg^{-1}) and power (90 W kg^{-1}) density values [49].

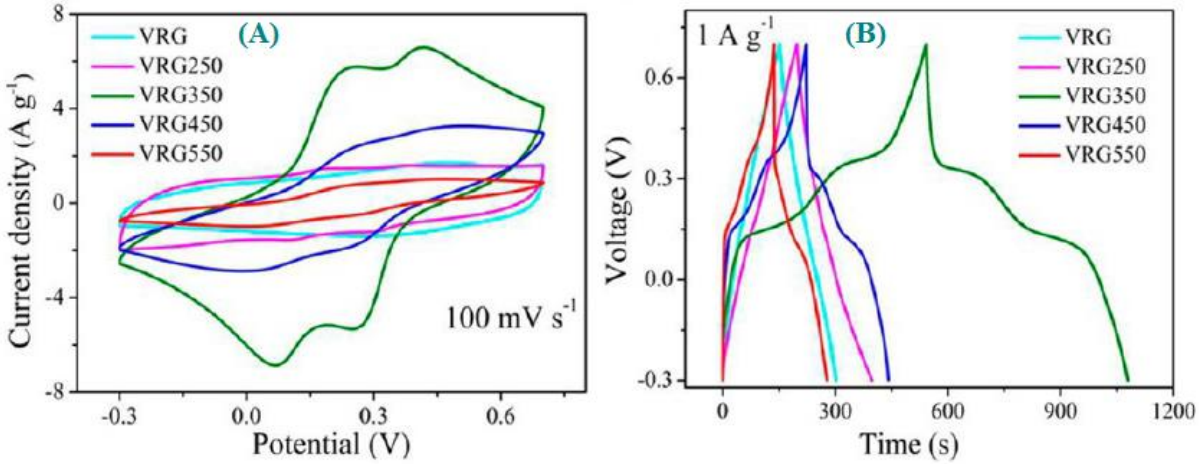

Figure 2. ("Reprinted with permission from (ACS Appl. Mater Interfaces 5 *(2013) 11462-11470*). Copyright (2013) American Chemical Society") Ref [54].

A hierarchical cobalt oxide/cobalt hydroxide ($Co_3O_4/Co(OH)_2$) nanoflakes electrode has been developed for electrochemical capacitance (601 F g^{-1}), the applied scan rate of 2 mV s^{-1} [50]. A one-dimensional growth of vanadium oxide supported polypyrrole (V_2O_5/Ppy) composite is a good candidate for supercapacitor and its displayed specific capacitance of 412 F g^{-1} from -1.4 to 0.6 V *vs* SCE [51]. On the other hand, hydrothermal preparation of CoO nanocubes@3D porous carbon skeleton of the rose morphological composite is applied on supercapacitor and obtained excellent capacitance performance [52]. The versatile material of 2D MnO_2 supported carbon nanotube composite demonstrated in the potential application of energy storage devices (10-fold increases in specific capacitance) [53]. The cyclic voltammogram (CV) and galvanostatic charge/discharge techniques displayed the best specific capacitance behaviour (Fig.2(A) & (B)). The fabricated V_2O_5/reduced graphene oxide (rGO) nanocomposite has been widely studied in a device, which exhibited a higher specific capacitance (537 F g^{-1}) and better cyclic stability (1000 cycles) [54].

2.3. Supercapacitors based on conducting polymer electrode materials

Generally, pseudocapacitive (conducting polymer) electrode materials have higher charge storage capacity than others (carbon). Bora *et al* [55] prepared a sulfonated graphene-based polypyrrole (SG/Ppy) nanocomposite via interfacial polymerization, which showed a higher specific capacitance value (360 F g^{-1}) and better cycling stability (500). Polyaniline-coated graphite nanofiber widely used in symmetric supercapacitor and it is attracted growing attention because of its best reversible capacity (2136 F g^{-1}), maximum energy density (24 Wh kg^{-1}) and power density (6000 W kg^{-1}), respectively [56]. Polyaniline hollow spheres (PANI-HS) supported electrochemically reduced graphene oxide (ERGO) hybrid core-shell composite provided greatly enlarged the specific surface area, high electroactive region and short lengths for both charge and ion transport [57]. A free-standing and flexible graphene/polyaniline composite sheets as building blocks with favourable tensile strength (12.6 MPa) and large electrochemical capacitances (233 Fg^{-1} for gravimetrically and 135 Fg^{-1} for volumetrically) [58]. Suppes *et al* [59] have used a porous polypyrrole/phosphomolybdate composite displayed high specific capacitance and low ionic resistance.

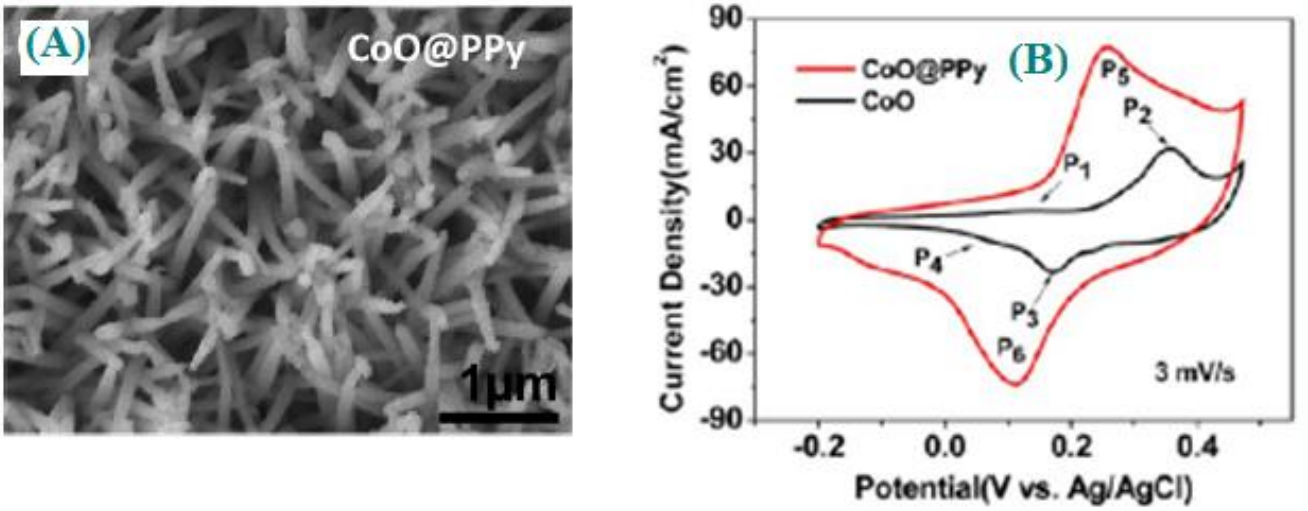

Figure 3. ("Reprinted with permission from (Nano. Lett 13 *(2013) 2078-2085*). Copyright (2013) American Chemical Society") Ref [60].

The hybrid material could increase their porosity, ionic conductivity, excellent reversibility and good cyclic stability. Figure.3(A) shows the low magnification SEM image of CoO@polypyrrole hybrid exhibited nanowire array surface wrinkled morphology and Fig.3(B) the optimized electrochemical performance of 3D hybrid (CoO@polypyrrole) nanowire electrodes were tested by cyclic voltammetric technique. The promising electrode materials are exhibited pseudocapacitive with excellent performance and cycling life [60]. Specifically, design and fabrication of core-double-shell carbon nanotube@polypyrrole@MnO_2 sponge can serve as a freestanding and compressible electrode for supercapacitor applications. In this core-double-shell a component making it straightforward mechanism study for structural optimization and enhanced good performances in supercapacitor applications [61]. In particular, polyaniline-camphorsulfonic acids (PANI/CSA) exhibited electrochemical capacitance value of 361 F g^{-1} @ 0.25 Ag^{-1} [62]. The design and development of three

different less-integrated graphene foam (graphene foam+Co_3O_4/poly(3,4-ethylenedioxythiophene)-MnO_2) porous nanostructures electrode can effectively improve by the superior electrochemical properties [63].

2.4. Supercapacitor based on nanocomposite electrode materials

Nanocomposites are excellent materials being developed for a wide range of applications such as electronics, electrochemical (electrochemical sensors, biosensors and energy storage devices) and military defence systems. The large surface area (1700 m^2 g^{-1}), great electrode potential and excellent electrochemical capacitance (237 F g^{-1}) of carbon precursor/CNT core-shell structure materials have been used as the best an electrode efficiently for supercapacitor [64]. A uniform ultrathin layer by layer-self assembled multi-layer film (LBL-MF) composed of PANI/RGO bilayer composite showed volumetric capacitance value of 584 F g^{-1} @ 3.0 A cm^{-3} [65].

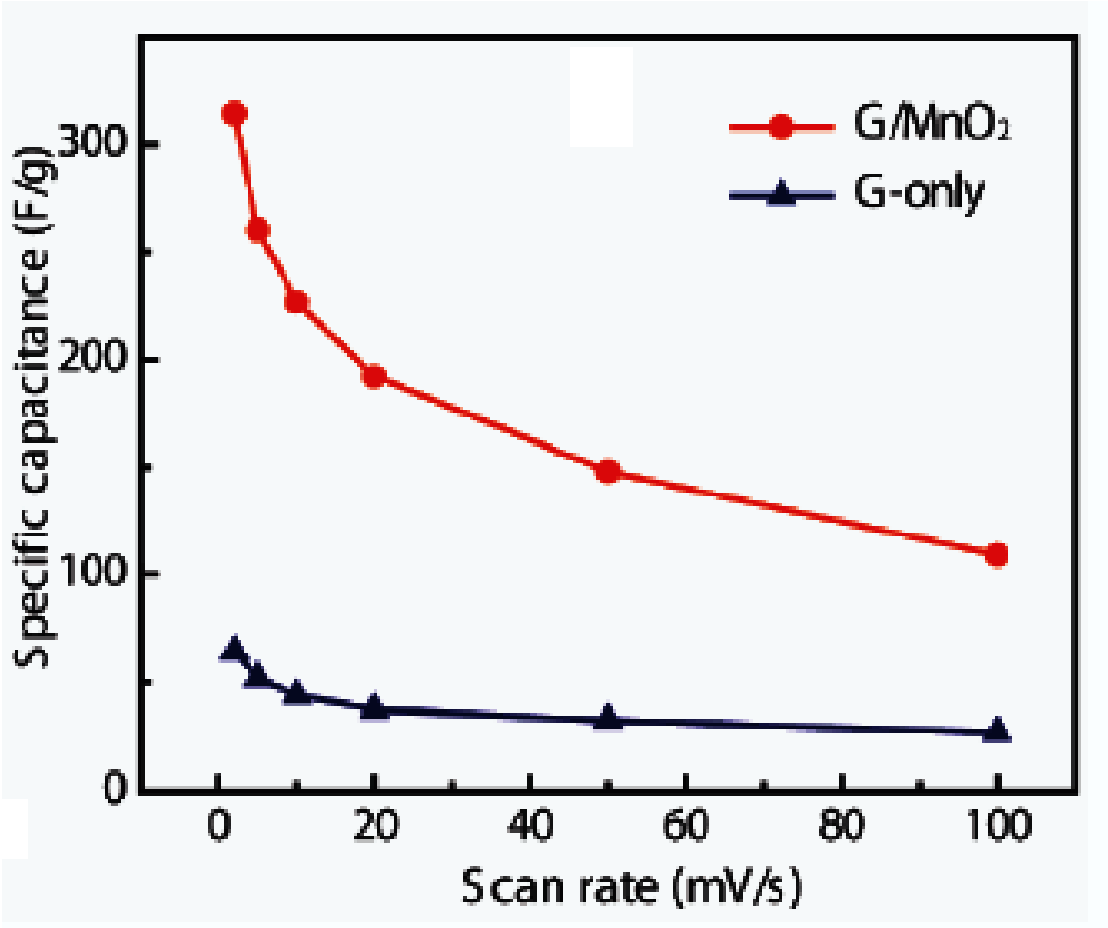

Figure 4. ("Reprinted with permission from (Nano. Lett 11 *(2011) 2905-2911*). Copyright (2011) American Chemical Society") Ref [71].

Dhibar *et al* [66] synthesized pure PANI, Ag-PANI and Ag-PANI/CNT nanocomposite displayed the specific capacitance value of 512 F g^{-1} @ 5 mV s^{-1} and better energy as well as power

density by in-situ polymerization techniques. Among the various asymmetric super capacitive materials, CNT/MnO_2/GR paper electrodes have attracted much attention due to efficient ionic, electronic transport, good electro capacitive, low-cost and environment friendliness [67]. Recently, chemically modified hybrid graphene nanosheet/Al^{2+}/Al^{3+} double hydroxide (GNS/LDH) supercapacitors have been made with a specific capacitance value of 781.5 F g^{-1} in 6.0M KOH solution [68]. Further, the abundant porous nanostructure of $Ni(OH)_2$-MnO_2-RGO ternary hybrid as the active electrode material is prepared by galvanostatic charge-discharge method, which attained the specific capacitance value of 1985 F g^{-1}[69]. A new class of potassium (K) incorporated nano graphitic structures have been regarded as the highly promising electrode, which results in the outer active sites increases with remarkable increased electrical conductivity [70]. The cyclic voltammogram of both modified graphene/MnO_2 textile and unmodified graphene nanosheets were recorded at different sweep rates (Fig.4). Hence, the modified electrodes highly desirable for high-performance electrochemical capacity tors, the achieved specific capacitance value of about 315 F g^{-1}[71]. A simple and cost-effective hydrogen-induced exfoliation method for the preparation of functionalized graphene-based PANI nanocomposites offer a fast electron transfer rate and enhance good capacitive (375 F g^{-1}) behaviour [72].

3. MORPHOLOGICAL STUDIES

A thin and free-standing CNT mesh/PANI composite showed uniform, oriented and nanoporous structure in the plane direction. In this well-constructed composite can exhibit many pores and may have great potential applications in flexible energy storage devices [73]. Herein, a novel intimately interconnected network like the morphological structure of V_2O_5 nanoporous has been widely investigated their achieved specific capacitance (316 F g^{-1}), rate capability, high energy density and superior long-term durability (Fig.5) [74]. In particularly, the nanoporous carbon materials resulting from the straightforward multi-template carbonization method and delivered specific capacitance of 236.5 F g^{-1} at 1 Ag^{-1} [75]. Recently, three-dimensional nanoporous ultra-thin $Ni(OH)_2$ supported ultrathin graphite foam (UGF) composite exploit their conductivity and the resulting the nanoporous structures offered high power energy storage [76]. Deori *et al* [77] reported better characteristics achieved by nanoporous Co_3O_4 with specific capacitance value ~ 476 F g^{-1} at the electrochemically active surface area of 289 m^2 g^{-1}. Single-crystal vanadium pentoxide (V_2O_5) nanorod arrays obtained from $VOSO_4$ by an electrochemical deposition method, with their length of about 10 mm, the diameter ranges from 100-200 nm and reported that nanorod arrays achieved significantly higher energy storage density [78]. Crumbled and rippled morphological structure of Bi_2S_3-graphene composite is demonstrated better capacitance (290 F g^{-1}) [79].

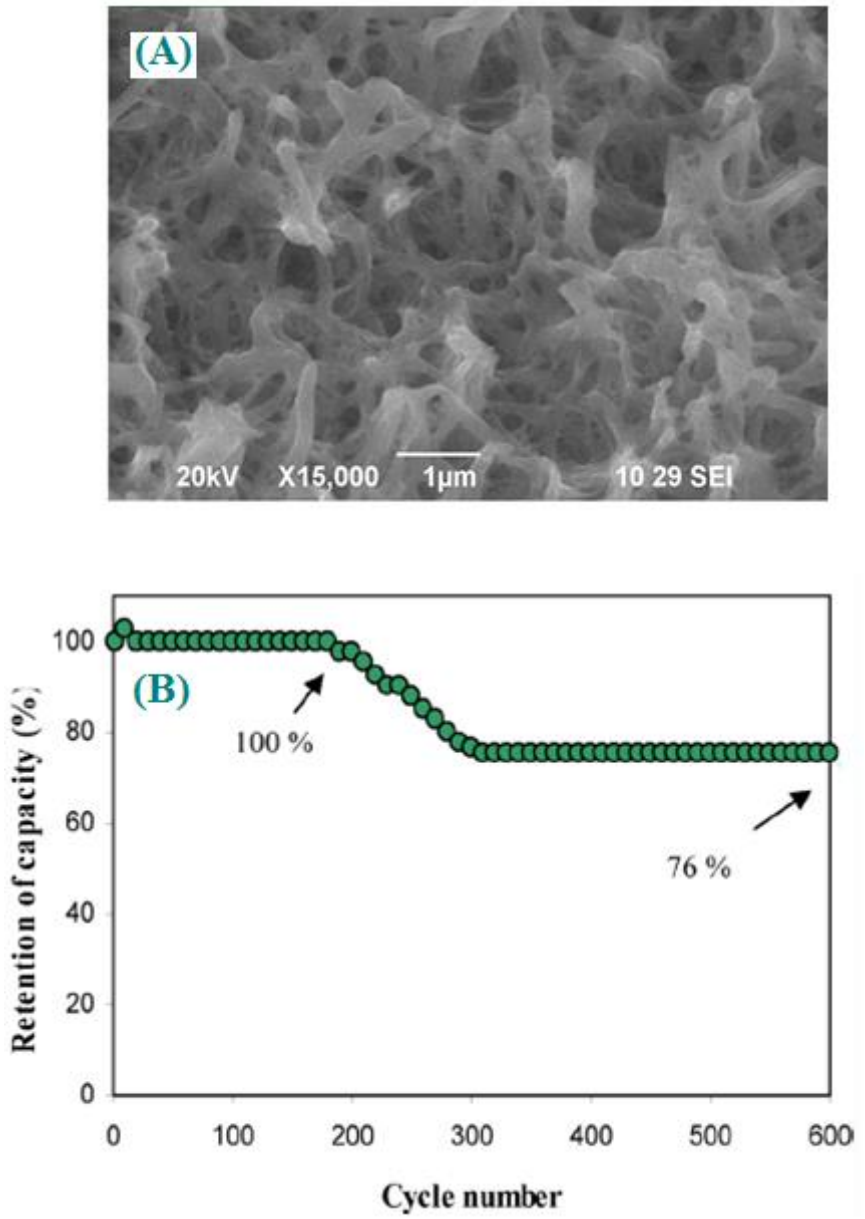

Figure 5. ("Reprinted with permission from (ACS Appl. Mater Interfaces 4 *(2012) 4484-4490*). Copyright (2012) American Chemical Society") Ref [74].

4. ANALYTICAL STUDIES

The electroanalytical technique is one of the significant techniques to give useful information's about the device of electrochemical reactions. Cho *et al* [80] reported the incorporation of highly porous polyaniline thin film electrode by the solution-based method. The resultant cyclic voltammetry curves displayed at different electrodes, benzoyl peroxide (BPO) modified PANI composite exhibited higher electrochemical performances (361 F g^{-1}). Amine-supported reduced graphene oxide-based PANI (H_2N-RGO/PANI) composites have shown higher capacitance than RGO/PANI, N-RGI/PANI and GO/PANI [81]. Rakhi *et al* [82] reported an economical and scalable electrodeposition of hydrous RuO_2 nanoparticles dispersed on mesoporous cobalt oxide (Co_3O_4) nanosheet electrode array for supercapacitor applications. They could achieve an excellent specific capacitance of 905 F g^{-1} @ 1 A

g^{-1}. Nanoflakes of NiO enhanced the diffusion layer and provide better charge (slow charge and fast discharge) storage capabilities (401 F g^{-1}) [83]. Lacey reduced graphene oxide nanoribbons (LRGONR) have been extensively studied in recently due to enhanced the electrocatalytic accessibility and showed the ultrahigh performance of specific capacitance [84]. The extensive studies of highly efficient 1-dimensional flexible stainless steel mesh (SSM) supported MnO_2 electrode have focused on electrode geometry, good rate capability and their supercapacitor specific capacitance properties studies using electrochemical impedance spectroscopy and galvanostatic charge/discharge study as shown in Fig.6 [85].

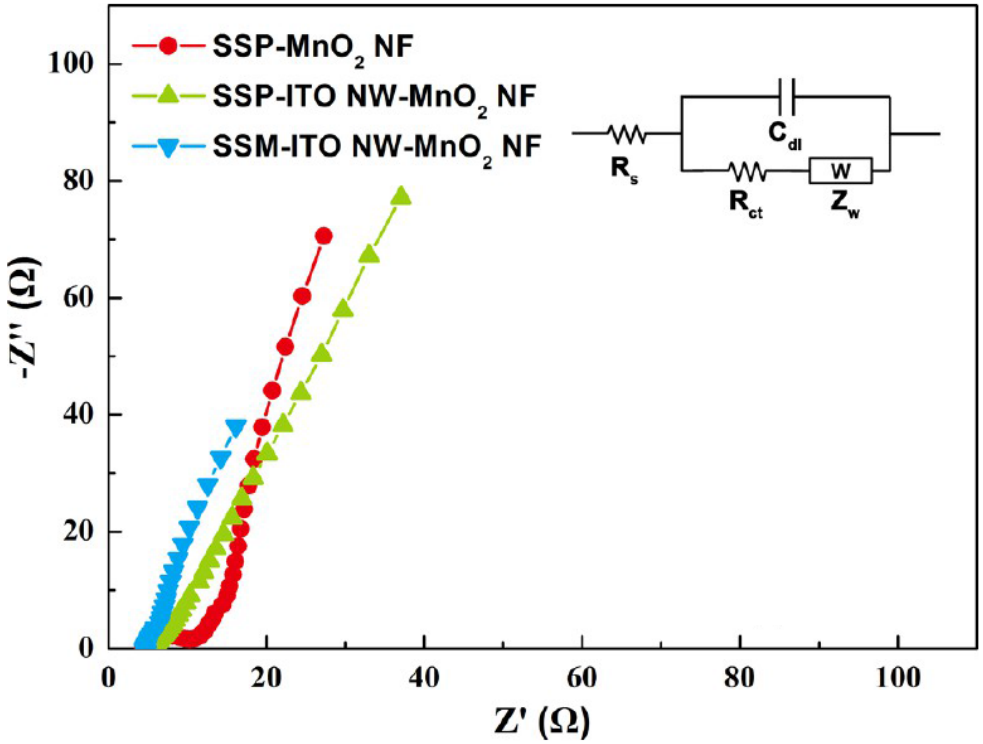

Figure 6. ("Reprinted with permission from (ACS Appl. Mater Interfaces 6 *(2014) 268-274*). Copyright (2014) American Chemical Society") Ref [85].

5. ELECTRODE STABILITY

The development of novel $NiCo_2O_4$@$NiCo_2O_4$ core/shell nanoflake array based high-performance supercapacitor grown on nickel foam. Figure.7. shows the fabricated core/shell nanoflake arrays achieved the specific capacitance value of 1.55 cm^{-2} and superior electrode cyclic stability (4000 cycles) [86]. Zhang *et al* [87] prepared uniform graphene nanoparticles supported copper ferrate ($CuFe_2O_4$-GN) nanocomposite hold great promise electrochemical capacitance (576.6 F g^{-1} @ 1 Ag^{-1}) applications. The composite showed remarkable synergetic effect between $CuFe_2O_4$ and graphene, it is exhibited good rate performance and long-term durability during the charge-discharge process. A novel flexible hybrid reduced graphene oxide (RGO) rapped with polyaniline (PANI) nanowire array deposited on nitrogen-doped carbon fibre cloth (eCFC) exhibited a specific capacitance of 1145 F g^{-1}, as reported by Yu *et al* [88]. The three-dimensional (3D) supported ultrathin derived graphene (UDG)

hybrid deposited on Ni foam, which provides a better pseudocapacitive performance (425 F g^{-1}) and good capacitive retention (90 %) [89].

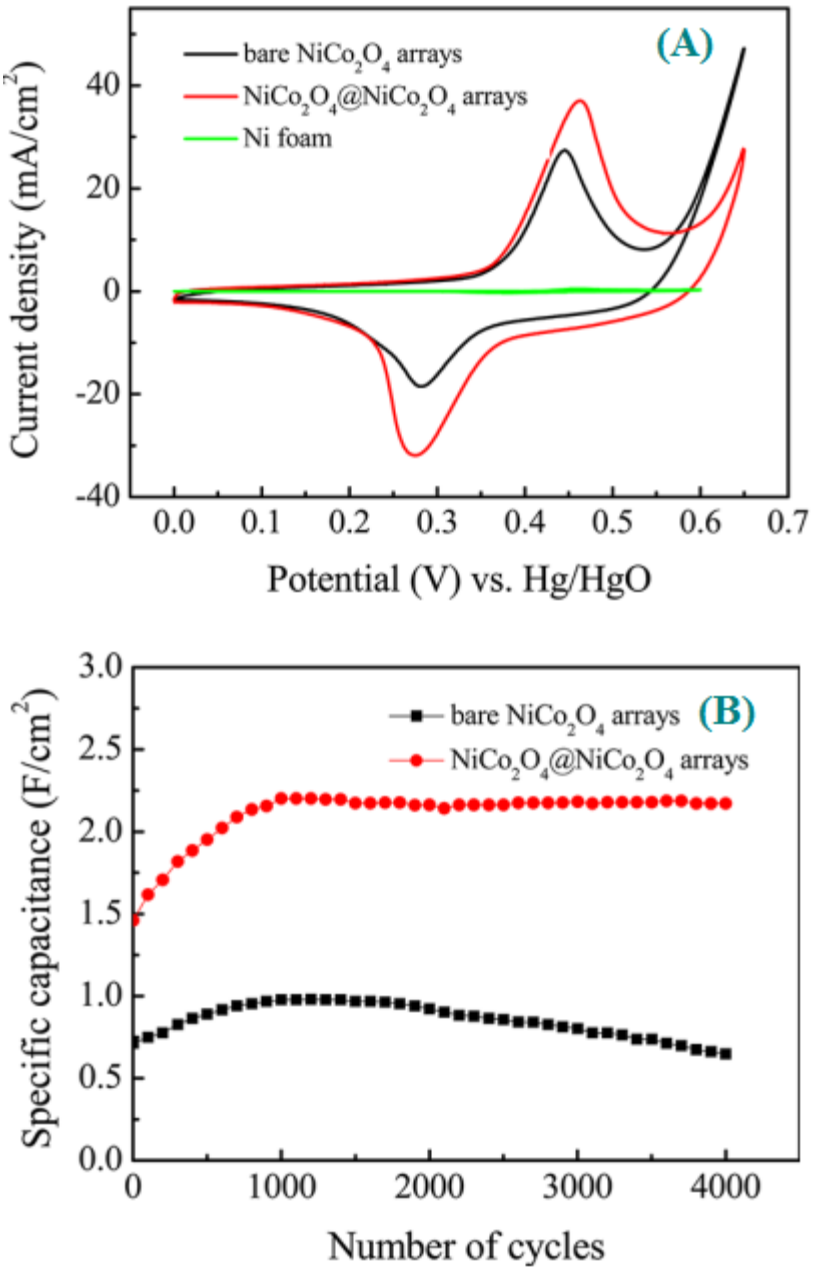

Figure 7. ("Reprinted with permission from (ACS Appl. Mater Interfaces 5 *(2013) 8790-8795*). Copyright (2013) American Chemical Society") Ref [86].

Feng *et al* [90] have used a flexible, ultrathin, lightweight and portable high performance of electrochemical storage device, the asymmetric porous MnO_2 grown on conducting paper (Ni/graphite/paper) can act as a negative electrode and $Ni(OH)_2$ grown on NGP as the positive electrode. The fabricated asymmetric paper supercapacitors (APSCs) displayed high specific capacitance (C_{sp}) (3.05 F cm^{-3}) and superior cyclic stability.

6. CONCLUSIONS

Up to date focused on the recent development has been made in inexpensive and eco-friendly synthesis route to the preparation of novel based different morphological electrode materials for the breakthrough in the field of supercapacitor applications. And also in this article, we have summarized various preparation methods, materials, different morphological studies and highly sensitive electrochemical analysis of supercapacitance performance. Among these, conducting polymer-based nanocomposite showed a high surface area and it could be a great benefit in the enhancement of specific capacitance values. The author mainly focused on catalytic properties, particles diameter (size), electrode surface area, morphology, catalytic activity and long term-durability, were reviewed in this article. There is a great inspiring and promising energy storage devices, the rapid progress and major impact of ultracapacitors may be in future.

ACKNOWLEDGEMENT
We take this opportunity to thank all of the co-workers of in our research groups who have contributed the collecting of research articles and also the author would like to thank Science & Engineering Research Board (SERB), under the grant no. SERB/F/8355/2016-17 dated 16th February 2017, India.

References

1. Z. Zhao, Y. Sun, P. Li, W. Zhang, K. Lian, J. Hu, Y. Chen, *Talanta*, 158 (2016) 283-291.
2. S.S.J. Aravind, T.T. Baby, T. Arockiadoss, R.B. Rakhi, S. Ramaprabhu, *Thin solid films*, 519 (2011) 5667-5672.
3. Y. Li, W. Gao, L. Ci, C. Wang, P.M. Ajayan, *Carbon*, 48 (2010) 1124-1130.
4. G. Wang, D. Li, C.O. Too, G.G. Wallace, *Chem. Mater*., 21 (2009) 2604-2606.
5. Y. Zhang, H. Li, L. Pan, T. Lu, Z. Sun, *J. Electro Anal. Chem*., 634 (2009) 68-71.
6. K.R. Ratinac, W. Yang, S.P. Ringer, A.F. Bract, *Environ. Scie. Technol*., 44 (2010) 1167-1176.
7. A.G. Pandolfo, A.F. Hollenkamp, *J. Power Sources*, 157 (2006) 11.
8. G. Lota, K. Fic, E. Frackowiak, *Energy Environ. Sciences*, 4 (2011) 1592-1605.
9. M. Winter, R.J. Brodd, *Chem. Rev.,* 104 (2004) 4245.
10. M.S. Saha, Y. Zhang, M. Cai, X. Sun, *Int. J. Hydrogen Energy*, 37 (2012) 4633-4638.
11. Y. Zhang, J. Sun, Y. Hu, S. Li, Q. Xu, *J. Power sources*, 239 (2013) 169-174.
12. Q. Zhang, Z. Bai, M. Shi, L. Yang, J. Qiao, K. Jiang, *Electrochim. Acta*, DOI: 10.1016/J.electa.2015.01.207.
13. Y. Wang, Z. Shi, Y. Huang, Y. Ma, C. Wang, M. Chen, Y. Chen, *J. Phys. Chem* C, 113 (2009) 13103-13107.
14. A.K. Mishra, S. Ramaprabhu, *J. Phys. Chem*. C, 115 (2011) 14006-14013.
15. Y. Tan, C. Xu, G. Chen, Z. Liu, M. Ma, Q. Xie, N. Zheng, S. Yao, *ACS Appl. Mater Interfaces*, 5 (2013) 2241-2248.
16. T.M. Higgins, D. McAteer, J.C.M. Coelho, B.M. Sanchez, Z. Gholamvand, G. Moriarty, N. McEvoy, N.C. Berner, G.S. Duesbeg, V. Nicolosi, J.N. Coleman, *ACS Nano*, 8 (2014) 9567-9579.
17. X. Zhang, X. Wang, L. Jiang, H. Wu, J. Su, *J. Power Sources*, 216 (2012) 290-296.
18. X. Wang, X. Li, L. Zhang, Y. Yoon, P.K. Weber, H. Wang, J. Guo, H. Dai, *Science*, 324 (2009) 768-771.
19. J.X. Feng, S.H. Ye, X.F. Lu, Y.X. Tong, G.R. Li, *ACS Appl. Mater Interfaces*, 7 (2015) 11444-11451.

20. F.K. Butt, M. Tahir, C. Cao, F. Idrees, R. Ahmed, W.S. Khan, Z. Ali, N. Mahmood, M. Tanveer, A. Mahmood, I. Aslam, *ACS Appl. Mater Interfaces*, 6 (2014) 13635-13641.
21. D. Feng, Y. Lu, Z. Wu, Y. Dou, L. Han, Z. Sun, Y. Xia, G. Zheng, D. Zhao, *J. Am. Chem. Soc*., 133 (2011) 15148-15156.
22. G. Zheng, L. Hu, H. Wu, X. Xie, Y. Cui, *Energy Environ. Sicences*, 4 (2011) 3368-3373.
23. G. Milezarek, O. Inganas, *Science*, 335 (2012) 1468-1471.
24. M. Kim, J. Kim, *ACS Appl. Mater Interfaces*, 6 (2014) 9036-9045.
25. X. Meng, M. Zhou, X. Li, J. Yao, F. Liu, H. He, P. Xiao, Y. Zhang, *Electrochim. Acta*, 109 (2013) 20-26.
26. Y. Tang, Y. Liu, S. Liu, S. Yu, W. Guo, S. Mu, H. Wang, Y. Zhao, L. Hou, Y. Fari, F. Gao, *Electrochim. Acta*, 161 (2015) 279-289.
27. Y.H. Hsu, C.C. Li, C.L. Ho, C.T. Lo, *Electrochim. Acta*, 127 (2014) 369-376.
28. J.H. Lin, T.H. Lin, C.K. Pan, *Energy Fuels*, 23 (2009) 4668-4677.
29. Y. Tang, Y. Liu, S. Yu, W. Guo, S. Mu, H. Wang, Y. Zhao, L. Hou, Y. Fan, F. Gao, *Electrochim. Acta*, 161 (2015) 279-289.
30. B.H. Kim, K.S. Yang, J.P. Ferraris, *Electrochim. Acta*, 75 (2012) 325-331.
31. L. Yang, S. Cheng, Y. Ding, X. Zhu, Z.L. Wang, M. Liu, *Nano Lett.*, 12 (2012) 321-325.
32. W. Yu, W. Lin, X. Shao, Z. Hu, R. Li, D. Yuan, *J. Power Sources*, 272 (2014) 137-143.
33. S. Vadivel, A.N. Naveen, V.P. Kamalakannan, P. Cao, N. Balasubramanian, *Appl. Surface Science*, 351 (2015) 635-645.
34. C.J. Raj, B.C. Kim, W.J. Cho, S. Park, H.T. Jeong, K. Yoo, K.H. Yu, *J. Electroanal. Chem*., 747 (2015) 130-135.
35. Z.J. Zhang, L.X. Cheng, X.Y. Chen, *Electrochem. Acta*, 161 (2015) 84-94.
36. T. Aytug, M.S. Rager, W. Higgins, F.G. Brown, G.M. Veith, C.M. Rouleau, H. Wang, Z.D. Hood, S.M. Mahurin, R.T. Mayes, P.C. Joshi, T. Kuruganti, *ACS Appl. Mater Interfaces*, 10 (2018) 11008-11017.
37. X. An, T. Simmons, R. Shah, C. Wolfe, K.M. Lewis, M. Washington, S.K. Nayak, S. Talapatra, S. Kar, *Nano Lett*., 10 (2010) 4295-4301.
38. S. Ye, J. Feng, P. Wu, *ACS Appl. Mater Interfaces*, 5 (2013) 7122-7129.
39. Y. Tan, C. Xu, G. Chen, Z. Liu, M. Ma, Q. Xie, N. Zheng, S. Yao, *ACS Appl. Mater Interfaces*, 5 (2013) 2241-2248.
40. H. Sun, W. He, C. Zong, L. Lu, *ACS Appl. Mater Interfaces*, 5 (2013) 2261-2268.
41. L.F. Chen, X.D. Zhang, H.W. Liang, M. Kong, Q.F. Guan, P. Chen, Z.Y. Wu, S.H. Yu, *ACS Nano*, 6 (2012) 7092-7102.
42. Z. Lei, F. Shi, L. Lu, *ACS Appl. Mater Interfaces*, 4 (2012) 1058-1064.
43. T.M. Higgins, D.M. Ateer, J.C.M. Coelho, B.M. Sanhez, Z. Gholamvand, G. Moriarty, N.M. Evoy, N.C. Berner, G.S. Duesberg, V. Nicolosi, J.N. Coleman, *ACS Nano*, 8 (2014) 9567-9579.
44. M. Kim, J. Kim *ACS Appl. Mater Interfaces*, 6 (2014) 9036-9045.
45. X. Zheng, X. Yan, Y. Sun, Z. Bai, G. Zhang, Y. Shen, Q. Liang, Y. Zhang, *ACS Appl. Mater Interfaces*, 7 (2015) 2480-2485.
46. Y. Lei, J. Li, Y. Wang, L. Gu, Y. Chang, H. Yuan, D. Xiao *ACS Appl. Mater Interfaces*, 6 (2014) 1773-1780.
47. Y. Tian, S. Cong, W. Su, H. Chen, Q. Li, F. Geng, Z. Zhao, *Nano Lett.*, 4 (2014) 2150-2156.
48. X.C. Dong, H. Xu, X.W. Wang, Y.X. Huang, M.B.C. Park, H. Zhang, L.H. Wang, W. Huang, P. Chen, *ACS Nano*, 6 (2012) 3206-3213.
49. P. Tang, L. Han, L. Zhang, *ACS Appl. Mater Interfaces*, 6 (2014) 10506-10515.
50. M. Oorbani, N. Naseri, A.Z. Moshfegh, *ACS Appl. Mater Interfaces*, 7 (2015) 11172-11179.
51. M.h. Bai, L.J. Bian, Y. Song, X.X. Li, *ACS Appl. Mater Interfaces*, 6 (2014) 12656-12664.
52. D. Lan, Y. Chen, P. Chen, X. Chen, X. Wu, X. Pu, Y. Zeng, Z. Zhu *ACS Appl. Mater Interfaces*, 6 (2014) 11839-11845.

53. T.M. Higgins, D. McAteer, J.C.M. Coesho, B.M. Sanchez, Z. Gholamvand, G. Moriarty, N. Mcevoy, N.C. Berner, G.S. Duesberg, V. Nicolosi, J.N. Colomen, *ACS Nano*, 8 (2014) 9567-9579.
54. M. Li, G. Sun, P. Yin, C. Ruan, K. Ai, *ACS Appl. Mater Interfaces*, 5 (2013) 11462-11470.
55. C. Bora, J. Sharma, S. Dolui, *J. Phys. Chem*. C, 118 (2014) 29688-29694.
56. X. Li, L. Yang, Y. Lie, L. Gu, D. Xiao, *ACS Appl. Mater Interfaces*, 6 (2014) 19978-19989.
57. W. Fan, C. Zhang, W.W. Tjiu, K.P. Pramoda, C. He, T. Liu, *ACS Appl. Mater Interfaces*, 5 (2013) 3382-3391.
58. D.W. Wang, F. Li, J. Zhao, W. Ren, Z.G. Chen, J. Tan, Z.S. Wu, I. Gentle, G.Q. Lu, H.M. Cheng, *ACS Nano*, 3 (2009) 1745-1752.
59. G.M. Suppes, B.A. Deore, M.S. Freund, *Langmuir*, 24 (2008) 1064-1069.
60. C. Zhou, Y. Zhang, Y. Li, J. Liu, *Nano Lett*., 13 (2013) 2078-2085.
61. P. Li, Y. Yang, E. Shi, Q. Shen, Y. Shang, S. Wu, J. Wei, K. Wang, H. Zhu, A. Cao, D. Wu, *ACS Appl. Mater Interfaces*, 6 (2014) 5228-5234.
62. S. Cho, K.H. Shin, J. Jang, *ACS Appl. Mater Interfaces*, 5 (2013) 9186-9193.
63. X. Xia, D. Chao, Z. Fan, C. Guan, X. Cao, H. Zhang, H.J. Fan, *Nano Lett.*, 14 (2014) 1651-1658.
64. Y. Yao, C. Ma, J. Wang, W. Qiao, L. Ling, D. Long, *ACS Appl. Mater Interfaces*, (2015) 4817-4825.
65. A.K. Sarker, J.D. Hong, *Langmuir*, 28 (2012) 12637-12646.
66. S. Dhibar, C.K. Das, *Ind. Eng. Chem. Res*, 53 (2014) 3495-3508.
67. Y. Jin, H. Chen, M. Chen, N. Liu, Q. Li, *ACS Appl. Mater Interfaces*, 5 (2013) 3408-3416.
68. Z. Gao, J. Wang, Z. Li, W. Yang, B. Wang, M. Hou, Y. He, Q. Liu, T. Mann, P. Yang, M. Zhang, L. Liu, *Chem. Mater*., 23 (2011) 3509-3516.
69. H. Chen, S. Zhou, L. Wu, *ACS Appl. Mater Interfaces*, 6 (2014) 8621-8630.
70. S. Saha, M. Jana, P. Samanta, N.C. Murmu, T. Kuila, *Ind. Eng. Chem. Res*., 55 (2016) 11074-11084.
71. G. Yu, L. Hu, M. Vosgueritchian, H. Wang, X. Xie, J.R. McDonough, X. Cui, Y. Cui, Z. Bao, *Nano Lett*., 11 (2011) 2905-2911.
72. A.K. Mishra, S. Ramaprabhu, *J. Phys. Chem*. C, 115 (2011) 14006-14013.
73. Y. Yin, C. Liu, S. Fan, *J. Phys. Chem*. C, 116 (2012) 26185-26189.
74. B. Saravanakumar, K.K. Prushothaman, G. Muralidharan, *ACS Appl. Mater Interfaces*, 4 (2012) 4484-4490.
75. Y.Q. Zhu, H.T. Yi, X.Y. Chen, Z.H. Xiao, *Ind.Eng.Chem. Res*., 54 (2015) 4956-4964.
76. J. Ji, L.L. Zhang, H. Ti, Y. Li, X. Zhao, X. Bai, X. Fan, F. Zhang, R.S. Ruoff, *ACS Nano*, 7 (2013) 6237-6243.
77. K. Deori, S.K. Ujjain, R.K. Sharma, S. Deka, *ACS Appl. Mater Interfaces*, 5 (2013) 10665-10672.
78. K. Takahasi, S.J. Limmer, Y. Wang, G. Cao, *J. Phys.Chem*. B, 108 (2004) 9795-9800.
79. S. Vadivel, A.N. Naveen, V.P. Kralakannan, P. Cao, N. Balasubramanian, *Appl. Surface Science*, 351 (2015) 635-645.
80. S. Cho, K.H. Shin, J. Jang, *ACS Appl. Mater Interfaces*, 5 (2013) 9186-9193.
81. L. Lai, Y. Yang, L. Wang, B.K. The, J. Zhong, H. Chou, L. Chen, W. Chen, Z. Shen, R.S. Ruoff, J. Lin, *ACS Nano*, 6 (2012) 5941-5951.
82. R.B. Rakhi, W. Chen, M.N. Hedhili, D. Cha, H.N. Alshareef, *ACS Appl. Mater Interfaces*, 6 (2014) 4196-4206.
83. S. Vijayakumar, S. Nagamuthu, G. Muralidharan, *ACS Appl. Mater Interfaces*, 5 (2013) 2188-2196.
84. V. Sahu, S. Shekhar, R.K. Sharma, G. Singh, *ACS Appl. Mater Interfaces*, 7 (2015) 3110-3116.
85. J.S. Kim, S.S. Shin, H.S. Han, L.S. Oh, D.H. Kim, J.H. Kim, K.S. Hong, J.Y. Kim, *ACS Appl. Mater Interfaces*, 6 (2014) 268-274.
86. X. Liu, S. Shi, Q. Xiong, L. Li, Y. Zhang, H. Tang, C. Gu, X. Wang, J. Tu, *ACS Appl. Mater Interfaces*, 5 (2013) 8790-8795.

87. W. Zhang, B. Quan, C. Lee, S.K. Park, X. Li, E. Choi, G. Diao, Y. Piao, *ACS Appl. Mater Interfaces*, 7 (2015) 2404-2414.
88. P. Yu, Y. Li, X. Zhao, L. Wu, Q. Zhang, *Langmuir*, 30 (2014) 5306-5313.
89. C.H. Wu, S. Deng, H. Wang, Y.X. Sun, J.B. Liu, H. Yan *ACS Appl. Mater Interfaces*, 6 (2014) 1106-1112.
90. J.X. Feng, S.H. Ye, X.F. Lu, Y.X. Tong, G.R. Li, *ACS Appl. Mater Interfaces*, 7 (2015) 11444-11451.